Efficient and accurate treatment of weak pairs in local CCSD(T) calculations

Oliver Masur, Denis Usvyat, and Martin Schütz

Citation: The Journal of Chemical Physics **139**, 164116 (2013); doi: 10.1063/1.4826534
View online: http://dx.doi.org/10.1063/1.4826534
View Table of Contents: http://scitation.aip.org/content/aip/journal/jcp/139/16?ver=pdfcov
Published by the AIP Publishing

Efficient and accurate treatment of weak pairs in local CCSD(T) calculations

Oliver Masur, Denis Usvyat, and Martin Schütz[a)]
Institut für Physikalische und Theoretische Chemie, Universität Regensburg, Regensburg D-93040, Germany

(Received 1 August 2013; accepted 9 October 2013; published online 28 October 2013)

Local coupled cluster theory is based on (i) a restriction of the list of pairs (or triples) of occupied molecular orbitals, and (ii) a truncation of the virtual space to orbital pair (or triple) specific subspaces. The latter is motivated by an exponential decay of the contributions to the pair energy with respect to the distance between related local occupied and virtual orbitals; the former only by a polynomial R^{-6} decay with respect to the distance R between the two occupied orbitals of the pair. Consequently, the restriction of the pair list is more critical, and contributions of pairs should not be neglected unless the corresponding interorbital distance is really large. In local coupled cluster theory pairs are usually discriminated on the basis of the interorbital distance, or the size of the 2nd order Møller-Plesset perturbation theory (MP2) estimate of the pair energy. Only strong pairs are treated at the full coupled cluster level, while weak pairs are treated just at the level of MP2. Yet MP2 might be problematic in certain cases, for example, π-stacking is badly described by MP2, etc. We propose to substitute the MP2 treatment of weak pairs by an approach based on ring-CCD by including third-order diagrams with R^{-6} decay behavior. Such an approach is clearly superior; it provides higher accuracy, while the computational cost is not significantly higher than that of a MP2 based treatment of weak pairs. © *2013 AIP Publishing LLC*. [http://dx.doi.org/10.1063/1.4826534]

I. INTRODUCTION

Coupled Cluster (CC) theory is probably the most successful *ab initio* electronic structure method to treat dynamic electron correlation effects.[1,2] The exponential wavefunction ansatz $|\mathrm{CC}\rangle = \exp(\mathbf{T})|\mathbf{0}\rangle$, where $\mathbf{T}$ is the cluster operator, and $|\mathbf{0}\rangle$ the reference (usually Hartree-Fock) determinant, ensures size extensivity. Moreover, it introduces all excited determinants of full configuration interaction (FCI) not covered by the truncated cluster operator $\mathbf{T}$ into $|\mathrm{CC}\rangle$, with coefficients factorized into products of amplitudes already included in $\mathbf{T}$. Truncated CC theory therefore can be regarded as an approximation to FCI based on a special tensor factorization of the FCI coefficients containing all FCI determinants. CC with singles and doubles substitutions, $\mathbf{T} = \mathbf{T}_1 + \mathbf{T}_2$, and an *a posteriori* perturbative treatment of triples substitutions, CCSD(T), has become the "Gold Standard" in quantum chemistry (this expression is attributed to Dunning). For single reference cases, chemical accuracy is reached with this method, provided that sufficiently large basis sets (eventually combined with basis set extrapolation techniques) are employed.

Canonical CCSD(T) has a computational cost of $\mathcal{O}(\mathcal{N}^7)$ relative to the molecular size $\mathcal{N}$, i.e., $\mathcal{O}(\mathcal{N}^6)$ for the iterative CCSD calculation, and $\mathcal{O}(\mathcal{N}^7)$ for the *a posteriori* perturbative triples correction (T). In order to defeat this unfavorably high scaling wall and to make the method also applicable to extended molecular systems, *local* CCSD(T) methods were developed during the past fifteen years.[3–9] The term "local" here implies the formulation of CCSD(T) in terms of spatially localized occupied and virtual molecular orbitals (MOs), rather than the commonly used delocalized and symmetry-adapted canonical orbitals diagonalizing the Fock matrix. Local MOs spanning the occupied space (LMOs) are usually obtained by applying a localization procedure such as Pipek-Mezey[10] or Boys[11] to the occupied canonical orbitals obtained from the preceding Hartree-Fock calculation. For the virtual space, e.g., projected atomic orbitals (PAOs),[12–17] orbital specific virtuals (OSVs),[6,18–21] or pair natural orbitals (PNOs)[22–29] can be used, either exclusively, or also in combination.

A formulation of CCSD(T) in terms of such local orbitals allows for a dramatic reduction of the determinants and related amplitudes entering the cluster operator $\mathbf{T}$, which is essentially based on (i) truncations of the virtual space, and (ii) pair approximations.[3,5,30] Truncations of the virtual space are enforced by allowing only, e.g., doubles substitutions from a certain LMO pair to PAOs in the immediate spatial vicinity of these two LMOs, or to OSVs related to either one of these two LMOs, or to PNOs related to this LMO pair. This is motivated by an exponential decay in the related amplitudes with respect to the distance between LMOs and local virtuals.

Pair approximations, on the other hand, discriminate individual LMO pairs and assign them to the pair classes of *strong*, *weak*, etc., pairs on the basis of their interorbital distance R: only *strong* pairs are treated at the CC level, while *weak* pairs are treated at a lower level of theory, typically at the level of second-order Møller-Plesset perturbation theory, MP2. A subset of weak pairs, denoted as *close* pairs, contribute, together with strong pairs, to the triples residual, and, optionally, to the (strong pair) doubles residual.

Pair approximations are motivated by the R^{-6} decay behavior of the individual pair energies with respect to the distance R between the respective LMOs, combined with perturbation theory arguments. It is assumed that the third- and

a)Electronic mail: martin.schuetz@chemie.uni-regensburg.de

higher order (within the MP partitioning) contributions to the weak pair energies are negligibly small. However, R^{-6} is a much weaker decay than the exponential one, that motivates truncations of the virtual space; the pair approximation hence has to be considered as more severe than the latter approximation. For example, it is well known that MP2 does not provide a sufficiently accurate description for the interaction between two π-stacked aromatic ring systems. MP2 often either underestimates (for systems with low polarizability) or overestimates (for systems with high polarizability) the interaction energies in intermolecular complexes and clusters.[31–34] Also, non-additive dispersion (Axilrod-Teller) contributions are not covered at the MP2 level. Hence, although many approximated CCSD schemes for extended systems explicitly[3–5,21,35,36] or implicitly[37] employ the MP2-like treatment for most of the pairs (similar to the weak pair approximation in the present context), it is questionable, if such a treatment provides in general sufficient accuracy.

In the present paper we investigate the accuracy of pair approximations for a set of diverse intermolecular complexes and clusters. On the basis of our results we propose to substitute the LMP2 treatment of weak pairs by a method based on ring-CCD[38–40] [ring-CCD is equivalent to the random phase approximation (RPA)[39,41]], with additional exchange terms such that the antisymmetry of the amplitudes in a spin-orbit formalism remains intact. In Sec. II we briefly outline the formalism of such a ring-CCD-based approach. In Sec. III we compare its performance, for a set of test systems, to the previous approach with weak pairs treated at the MP2 level. Section IV finally concludes this paper.

II. THEORY

In this section we first briefly define the general nomenclature and provide the CCSD residual equations for the strong pairs. Afterwards, the diagrams included in the different treatments of the weak pairs are discussed. As usual, indices i, j, k, l denote in the following localized occupied molecular orbitals (LMOs), while indices r, s, t, u denote localized virtual orbitals, i.e., PAOs. For other choices of localized virtuals like OSVs or PNOs the formulae are very similar and straightforwardly obtained from those presented here for PAOs.

A. The LCCSD residual for strong pairs

The LCCSD residual, defining the equations to be solved for the strong pair amplitudes, is given by

$$r_r^i = \left\langle \tilde{\Phi}_i^r \middle| e^{-\hat{T}} \hat{H} e^{\hat{T}} |\Phi_0\right\rangle = 0;\ \forall\, i; r \in [ii], \tag{1}$$

$$R_{rs}^{ij} = \left\langle \tilde{\Phi}_{ij}^{rs} \middle| e^{-\hat{T}} \hat{H} e^{\hat{T}} |\Phi_0\right\rangle = 0;\ \forall\, ij \in \{s\}; r, s \in [ij], \tag{2}$$

with $\hat{H} = \hat{F} + \hat{V}$ the normal ordered Hamiltonian (consisting of Fock operator $\hat{F}$ and fluctuation potential $\hat{V}$), $\hat{T} = \hat{T}_1 + \hat{T}_2$ with

$$\hat{T}_1 = \sum_i \sum_{r\in[ii]} t_r^i \hat{E}_{ri}, \tag{3}$$

$$\hat{T}_2 = \frac{1}{2} \sum_{ij\in\{s\}} \sum_{rs\in[ij]} T_{rs}^{ij} \hat{E}_{ri} \hat{E}_{sj}, \tag{4}$$

$|\Phi_0\rangle$ the Hartree-Fock reference wavefunction, and $\langle\tilde{\Phi}_i^a|$, $\langle\tilde{\Phi}_{ij}^{ab}|$ the contravariant configuration state functions,

$$\left\langle \tilde{\Phi}_i^r \right| = \frac{1}{2} \langle \Phi_0 | \hat{E}_{ri}^\dagger, \tag{5}$$

$$\left\langle \tilde{\Phi}_{ij}^{rs} \right| = \frac{1}{6} \langle \Phi_0 | (2\hat{E}_{ri}^\dagger \hat{E}_{sj}^\dagger + \hat{E}_{rj}^\dagger \hat{E}_{si}^\dagger), \tag{6}$$

used for projection. The $\hat{E}_{ri}$ denote spin-conserving one-particle excitation operators, and the t_r^i and T_{rs}^{ij} are the singles and doubles amplitudes, respectively.

Note that in Eqs. (1)–(4) the ranges of virtuals are restricted to "pair domains" $[ij]$, related to individual LMO pairs ij (in case of singles a diagonal pair). The detailed construction of these pair domains of course depends on the choice of the virtuals, i.e., whether PAOs, OSVs, or PNOs are employed. Furthermore, and what is of greater relevance for the present discussion, in Eqs. (2) and (4) the range of LMO pairs ij is restricted to the list of strong pairs $\{s\}$. As already mentioned in the Introduction, the assignment of the individual pairs to the distinct pair classes (strong, weak, distant) is usually done on the basis of the LMO interorbital distances, or connectivities.[5,30] In the latter case just the number of bonds between two LMOs is counted. Alternatively, it would also be possible to assign individual pairs to pair classes on the basis of the respective pair energies of, e.g., a preliminary MP2 calculation comprising all pairs.

In the present work we employed an assignment on the basis of distances: each LMO specifies its own subset of relevant atoms. This is obtained from a Löwdin population analysis by truncating the ordered atoms list beyond a certain population. The LMO distance then is defined as the distance between the two closest atoms of the two respective atom subsets. Typically, only LMO pairs with mutual overlapping atom subsets are considered as strong. Sometimes also enlarged strong pair lists with distances up to 3 bohrs are employed. The amplitudes of the remaining pairs are usually calculated at the level of MP2. To this end, the LMP2 amplitude equations,

$$R_{rs}^{ij} = \left\langle \tilde{\Phi}_{ij}^{rs} \middle| \hat{V} + [\hat{F}, \hat{T}_2] |\Phi_0\right\rangle = 0;\ \forall\, ij \in \{\mathrm{sw}\}; r, s \in [ij], \tag{7}$$

are ordinarily calculated initially (before the actual LCCSD calculation) for all pairs $ij \in \{\mathrm{sw}\}$ (strong + weak). The strong pairs are subsequently refined by solving the LCCSD equations (1) and (2).

Optionally, some of the weak pair LMP2 amplitudes (belonging to the subset of *close pairs*) can enter these equations and so couple with the strong pair amplitudes. In other words, the sum over ij pairs in Eq. (4) now runs over the combined list of strong and close pairs $\{sc\} = \{s\} \cup \{c\}$, rather than just over $\{s\}$. Actually, as demonstrated in Sec. III, it is indeed highly advisable to do this. On the other hand, strong pair amplitudes can only contribute to the LMP2 residual (7) via the term involving the Fock operator $\hat{F}$. Since the matrix representation

of the latter is diagonally dominant these couplings are very weak and can be neglected. Therefore, no further iteration beyond the initial LMP2 calculation is necessary.

Finally, after convergence of the LCCSD equations (1) and (2) for strong pairs also an *a posteriori* local triples correction L(T), or L(T0) can be evaluated. The corresponding formulae can be found in Refs. 3, 4, and 6, and are not reiterated here. We just mention at this point that strong and close pair amplitudes enter the triples residual.

B. The ring-CCD (rCCD) and rCCD3 residual for weak pairs

A LMP2 treatment of weak pairs of course is computationally very efficient. However, as already pointed out in the Introduction, it may not always provide satisfactory accuracy. In the course of the present work we have devised, implemented, and tested alternative methods for the treatment of these pairs, based on the ring-CCD (or rCCD for brevity) approach.

Several versions of ring-CCD were already considered in Refs. 39 and 40. The main motivation for the introduction of this approach in these papers is its equivalence to RPA. In particular, to preserve this equivalence the antisymmetry of the doubles amplitudes in spin-orbital basis with respect to permutation of the occupied or virtual indices is sacrificed. Yet in the present work we employ this method as an approximation to the CCSD method for weak pairs, without explicit reference to RPA, and therefore there is no need to drop the antisymmetry of the amplitudes. What is even more important, the corresponding diagrams, all absent in RPA, decay as slowly as the respective standard RPA-terms. At the same time, the additional computational effort to evaluate these terms is negligible compared to a standard RPA calculation. Hence, it is desirable to include them in the description of weak pairs.

In the CCD method the antisymmetry of the amplitudes is enforced by index permutation operators in the residual expression, introduced for non-equivalent external lines in the individual diagrams. Thus, we redefine the ring-CCD approximation such that the relevant index permutation operators in Eq. (7) of Ref. 39 are kept. Below we provide the diagrams and corresponding explicit expressions for such a ring-CCD ansatz in a spin-free closed-shell formalism. The rCCD residual, i.e., the amplitude equations are given by

$$R_{rs}^{ij} = \langle \tilde{\Phi}_{ij}^{rs} | \hat{V} + [\hat{H}, \hat{T}_2]_{\text{ring}} + [[\hat{H}, \hat{T}_2], \hat{T}_2]_{\text{ring}} | \Phi_0 \rangle = 0; \quad \forall\, ij \in \{\text{w}\}; r, s \in [ij], \tag{8}$$

where the subscript "ring" implies the restriction of the corresponding commutators to ring diagrams, maintaining all corresponding permutations operators.

We start from the approximation to rCCD, which we denote as *direct*-rCCD. The corresponding diagrams in the spin-free closed shell CC formalism are displayed in Fig. 1. It is related to *direct*-RPA, which disregards the exchange diagrams originating from the antisymmetry of the two-electron integrals in a spin-orbital formalism when going over to a spin-free formalism. Yet in contrast to direct-RPA (and generally RPA) the exchange terms originating from above mentioned antisymmetrized index permutations in the residual are kept (terms D3–D5). Furthermore, the weak pair energies are calculated via the standard CCD energy expression, which also includes the exchange terms (in this respect direct-rCCD is related to the second-order screened exchange [SOSEX] variant of direct-RPA[42]). Evaluation of such diagrams can be trivially combined with the diagrams D1 and D2 by using the transposed amplitude matrices for each pair. We note here that in the spin-orbital formalism the *direct*-rCCD amplitudes also lose the property of antisymmetricity with respect to index permutation. However, for the spin-free formalism employed in this work, where the amplitudes are not antisymmetric anyway, this does not lead to any implementational consequences (like doubling the number of unique amplitudes).

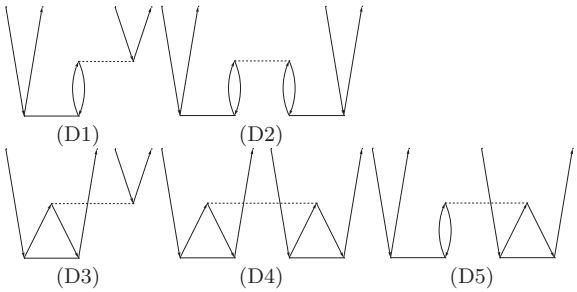

FIG. 1. Goldstone diagrams of *direct*-rCCD beyond MP2 (D1, D2) including additional exchange terms as obtained by transposition of respective amplitude matrix (D3–D5). The corresponding algebraic expressions are given in Table I.

Obviously, the strong pair amplitudes entering Eq. (8) no longer couple just via the Fock term as in LMP2, but also via terms involving the fluctuation potential. The reverse influence of the strong pair amplitudes on the rCCD residual thus is much stronger than on the LMP2 residual, and Eqs. (1), (2), and (8) have to be solved simultaneously in a common iterative procedure (just an initial rCCD calculation as in the case of LMP2 is entirely insufficient). Note that the rCCD residual (8) is restricted to weak pairs $ij \in \{\text{w}\}$, whereas the amplitudes entering it involve also strong pairs. On the other hand, as before,[3,5,30] only strong and close pair amplitudes enter the LCCSD residual (1,2), where close pairs constitute a certain subset of the list of weak pairs.

By virtue of density fitting[5,43–50] the *direct*-LrCCD diagrams plus exchange as shown in Fig. 1 can be evaluated very efficiently. For example, the first term of diagram D1 in Table I can be written as

$$R_{rs}^{ij} += \sum_P V_{rP}^i c_{sP}^j; \ \forall\, ij \in \{\text{w}\}; r, s \in [ij], \quad \text{with}$$

$$V_{rP}^i = \sum_{r' \in \cup[i]} S_{rr'} \sum_j \sum_{s \in [ij]} T_{r's}^{ij} (js|P); \ r \in \cup[i], \tag{9}$$

where $(js|P)$ are the three index electron repulsion integrals between the charge density js and the fitting function P, c_{rP}^i are the corresponding fitting coefficients, and $\cup[i]$ is the union of the pair domains $[ij]$ with common LMO i. The intermediate quantity V_{rP}^i is just the same as it appears in the DF-LMP2 gradient[51] and in DF-LCC2 linear response,[52,53] and can be calculated very efficiently.

TABLE I. Algebraic expressions for the Goldstone diagrams in Figs. 1 and 2 contributing to the weak pair residual R^{ij}_{rs}. For compactness Einstein's convention (implicit summation over repeated indices) is assumed. Electron repulsion integrals are given in Mulliken's notation. $S_{rr'}$ is an element of the metric of the (mutually not orthogonal) local virtuals. The respective weights of the diagrams are also given.

(D1)	+2	$S_{rr'}T^{ik}_{r't}(kt\|sj) + (ri\|kt)T^{kj}_{ts'}S_{s's}$
(D2)	+4	$S_{rr'}T^{ik}_{r't}(kt\|lu)T^{lj}_{us'}S_{s's}$
(D3)	−1	$S_{rr'}T^{ik}_{tr'}(kt\|sj) + (ri\|kt)T^{jk}_{ts'}S_{s's}$
(D4)	+1	$S_{rr'}T^{ik}_{tr'}(kt\|lu)T^{jl}_{us'}S_{s's}$
(D5)	−2	$S_{rr'}\left(T^{ik}_{r't}(kt\|lu)T^{jl}_{us'} + T^{ik}_{tr'}(kt\|lu)T^{lj}_{us'}\right)S_{s's}$
(D6)	−1	$S_{rr'}T^{ik}_{r't}(kj\|st) + (rt\|ki)T^{jk}_{s't}S_{s's}$
(D7)	−2	$S_{rr'}T^{ik}_{r't}(lt\|ku)T^{lj}_{us'}S_{s's}$
(D8)	+1	$S_{rr'}\left(T^{ik}_{tr'}(lt\|ku)T^{lj}_{us'} + T^{ik}_{r't}(lt\|ku)T^{lj}_{s'u}\right)S_{s's}$
(D9)	$-\frac{1}{2}$	$S_{rr'}T^{ik}_{tr'}(lt\|ku)T^{lj}_{s'u}S_{s's}$

The motive for the inclusion of the direct-rCCD diagrams depicted in Fig. 1 into the weak pair residual is that the their contribution to the pair energies decays with the interorbital distance at the same rate as MP2, i.e., as R^{-6}.[54] The leading order (within the MP partitioning) of the direct-rCCD terms in the energy though is higher; of third order for D1 and D3; and of 4th order for D2, D4, and D5. Unfortunately, as will be demonstrated in Sec. III, the performance of *direct*-LrCCD itself is rather poor; interaction energies are severely underestimated. Also the inclusion of above mentioned additional exchange diagrams, generated by a simple transpose of the amplitude matrices does not lead to an improvement. This disappointing behavior of *direct*-LrCCD was, in the course of the present work, attributed to the neglect of two further exchange diagrams of rCCD, which cannot be included so effortlessly as by a simple transpose of the amplitude matrices, but still decay not faster than R^{-6}. These two diagrams (D6, D7) are depicted in Fig. 2, along with those additional exchange diagrams (D8, D9) generated by transposition of the amplitude matrices in D7. The analogous exchange diagram originating from D6, is, in fact, equivalent to a ladder-diagram we intentionally omit due to reasons which become clear below. It is therefore not depicted in Fig. 2. D6 contributes to third, D7–D9 to fourth order in the correlation energy. D6–D9 are

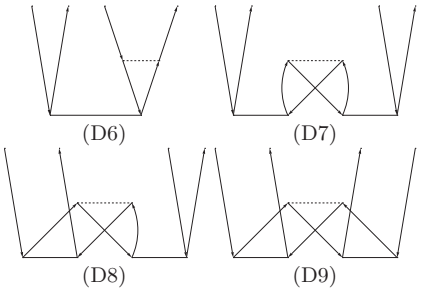

FIG. 2. Goldstone diagrams of the two additional exchange rCCD terms, not generated from the *direct*-rCCD ones by transposition of respective amplitude matrix (first column), and the diagrams, obtained by transposition of D7 (second column). The diagram obtained by transposition from D6 is grouped together with ladder diagrams (*vide infra*) and is thus not shown here. The algebraic expressions corresponding to the diagrams are given in Table I.

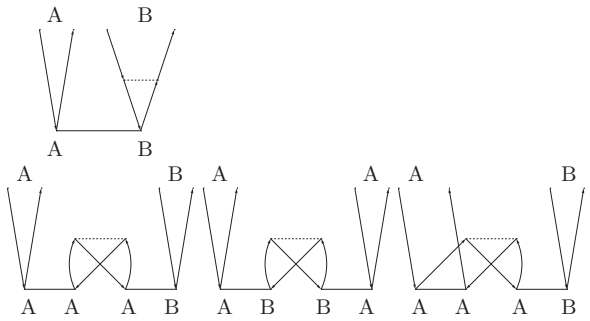

FIG. 3. Contributions of the Goldstone diagrams D6, D7, and D8, which decay as R^{-6} with the distance R between the two "remote" subsystems A and B containing the two LMOs of a close/weak pair.

related to the antisymmetry of the integrals in a spin-orbital formalism, hence an approach including these diagrams features the antisymmetry of the spin-orbit doubles amplitudes.

Diagrams D6–D8 indeed comprise energy contributions which decay as R^{-6} with the distance R between the two "remote" subsystems A and B containing the two LMOs of the weak pair. To see this, one can analyze the diagrams shown in Fig. 3. Consider a localized occupied $i, j, \ldots$ and virtual $r, s, \ldots$ orbital representation. Then a doubles amplitude T^{ij}_{rs} decays as R^{-3} with the distance between i and j (or r and s) and exponentially with distance between i and r or j and s, and so does the integral $(ir|js)$. The R^{-3} decay results from the strong orthogonality between the occupied and virtual manifold, giving rise to the dipole-dipole interaction as the leading term in the multipole approximation of the integral. The integral $(ij|rs)$, on the other hand, decays exponentially with ij-separation, and, generally, just as R^{-1} with the distance between the occupied and virtual orbitals (*vide infra*). The leading contribution to the energy originating from the open residual diagrams considered here is obtained by `bra`-side closure of these diagrams, implying contraction with an integral of $(ir|js)$-type, which imposes a further R^{-3}-decaying factor. With this in mind it is easy to see that the energy contributions from all the diagrams in Fig. 3 decay asymptotically as R^{-6}. For example, D6 comprises couplings of weak-pair amplitudes to weak-pair residuals via electron repulsion integrals $(k_B j_B|s_B t_B)$ entirely localized on subsystem B. D7, on the other hand, includes couplings between strong and weak pair amplitudes to weak pair residuals, as well as couplings between weak pair amplitudes and strong pair residuals. At the same time, the slowest possible decay of the energy contribution from the diagram of the D9-type is R^{-12}.

The ring approximation disregards the so called ladder diagrams (D10 and D11 of Fig. 4). The diagram D12 can

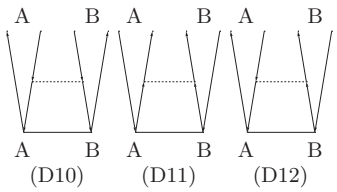

FIG. 4. Goldstone ladder diagrams omitted in rCCD. They altogether decay as R^{-9} with the distance R between the two "remote" subsystems A and B containing the two LMOs of the close/weak pair (see text).

also be considered as a ladder, but in fact can also be obtained from D6 by transposition of the amplitude matrices. These terms contribute in third order to the correlation energy and decay individually relatively slowly, i.e., just as R^{-7} (the integral decays as R^{-1}, since its orbital products are not chargeless). At the same time, these diagrams are computationally inconvenient, especially so D11 due to electron repulsion integrals involving four virtual orbitals, which constitute a very large integral distribution if the pair list comprises not only strong pairs. Fortunately, these diagrams can be omitted for the weak pairs altogether, since their overall contribution actually decays much quicker, namely, as R^{-9}.

To see this, consider the terms in a basis of localized orthonormal orbitals (this is always formally fulfilled; the LMOs or PNOs are indeed orthonormal, PAOs or OSVs can always be orthonormalized in the local basis forming, e.g., the appropriate pseudo canonical local basis). The R^{-4}-decaying contribution to the residual of a given pair then can only originate from ladder terms having orbital products in the integral with both occupied and both virtual orbitals being identical, i.e., diagonal terms. All other terms involve chargeless densities in the integral and consequently decay quicker. The sum of the three diagonal ladder terms with orbital products containing charge can then be combined into a single term with orbital products in the integral being equal to difference between the squared virtual and the squared occupied orbitals. By virtue of the normality of the orbitals the charge of such a orbital product difference again vanishes and the corresponding integral decays as R^{-3}. The overall contribution of the three ladder diagrams to the correlation energy hence decays as R^{-9}. A more detailed proof will be given in Ref. 54.

Finally, we analyze the 4th order CCD diagrams shown in Fig. 5, which do not enter the rCCD formalism. The energy contribution from the diagram D17 (Fig. 5) decays as quickly as R^{-12}, and, therefore this diagram can safely be omitted from the weak pair residual. The diagrams D13–D16, however, can provide a contribution which decays just as R^{-6}.

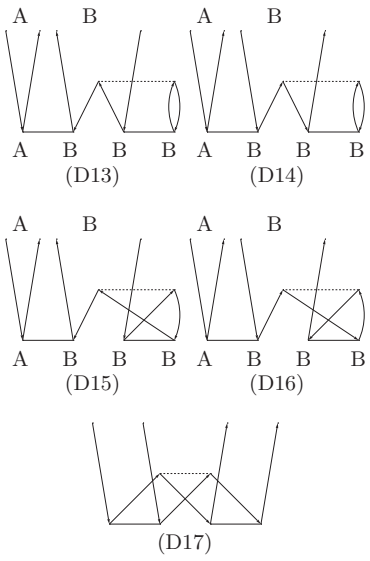

FIG. 5. Goldstone diagrams of the CCD 4th-order terms, absent in the rCCD formalism.

Hence their inclusion may provide a certain improvement in the description of weak pairs. These diagrams, however, are technically more difficult to evaluate efficiently and therefore were not considered in the present work. We defer an investigation of these 4th order diagrams to future work.

We also would like to mention, that in CCSD there are 5th-order diagrams, involving singles, with a very slow decay. When summed up they decay as slowly as R^{-3} (for monomers having dipoles). The energy contribution associated with these diagrams reflects the high-order electrostatic interactions between the monomers due to the correlated charge density corrections in each monomer. However, since these corrections are described by the intra-monomer amplitudes, these diagrams contribute to the strong pair residual and are thus naturally captured in LCCSD via the **G(E)** and the related internal term of Ref. 30 (see Eqs. (28) and (32) therein).

In the course of this work, it turned out that diagram D6 is of prime importance to improve on *direct*-LrCCD (d-LrCCD), whereas the effect of D7–D9 on interaction energies is tiny. In order to accommodate the missing exchange diagrams with R^{-6} decay, and in particular the third-order diagram D6, we implemented the full rCCD, as well as the third-order approximation to rCCD (rCCD3, which also could be denoted as ring-XCC(3),[55] ring-VCC[3],[56] or ring linearized CCD). rCCD3 comprises, apart from the MP2 diagrams, the diagrams D1 and D6. Density fitting was employed to factorize all diagrams apart from D6–D9. For D6 the set of required electron repulsion integrals $(kj|st)$ is fortunately rather compact. Indeed, since the integrals decay exponentially with the distance between LMOs k and j, or virtuals s and t, only strong pairs kj need to be considered in the evaluation of D6. Overall, the additional computational effort on going from a LMP2 to a rCCD3 treatment of weak pairs thus is rather modest (*vide infra*).

III. TEST CALCULATIONS

The accuracy of the different approaches for the treatment of close and weak pairs in LCCSD and LCCSD(T) calculations was tested by performing calculations on a set of diverse intermolecular complexes ranging from hydrogen bonded to van der Waals dominated systems. The geometries were taken from the S66 data set.[57] Furthermore, the Kr_3 and the $(CS_2)_3$ trimers were used as examples to test non-additive correlation contributions. Finally, to test the new rCCD3 approach for *intramolecular* close and weak pairs and to provide some comparative timings, calculations on a linear poly-glycine peptide chain $(Gly)_4$ were performed, for different specifications of the pair approximation, i.e., different numbers of strong, close, and weak pairs.

All calculations were performed in the aVTZ basis set (cc-pVTZ[58] on hydrogen atoms, aug-cc-pVTZ[59] on all other atoms). As auxiliary basis for density fitting appropriate MP2FIT basis sets of Weigend *et al.* were employed.[60]

In the calculations on the intermolecular complexes and clusters the local approximations (domains, pair lists, number of redundancies in the pair specific virtual spaces) were determined at large intermolecular separation and kept

fixed, as recommended for the treatment of intermolecular interactions.[61] Moreover, all intramolecular pairs were specified as strong, while all intermolecular pairs were specified as close (i.e., all intermolecular pairs are used in calculating the strong pair LCCSD and LCCSD(T) residuals), unless explicitly stated otherwise.

All calculations were performed with PAOs; excitation domains were constructed according to the Boughton-Pulay procedure[62] employing a completeness criterion of 0.985.

A. Intermolecular complexes from S66 data set

Table II compiles interaction energies E_{int}, their overall correlation contributions ΔE_{c}, as well as the intra- and intermolecular components δE_{intra}, and δE_{inter} thereof, for the test set of dimers. Pure LMP2 calculations, LCCSD calculations with LMP2 treatment of close pairs, LCCSD|LMP2, without and with coupling between close and strong pairs, as well as LCCSD|d-LrCCD, LCCSD|LrCCD3, and LCCSD|LrCCD calculations are compared to reference LCCSD calculations where all pairs (inter + intramolecular) are specified as strong.

The LMP2 interaction energies are for hydrogen bonded systems in quite good agreement with the LCCSD reference values, while for dispersion dominated, e.g., π-stacked systems the agreement is much worse and LMP2 generally overestimates. When breaking down the correlation contribution ΔE_{c} into δE_{intra} and δE_{inter} it becomes evident that LMP2 provides too low repulsive δE_{intra}. This is particularly so for the π-stacked systems; for example, for the pyridine dimer it amounts to 0.57 kcal/mol vs. 2.39 kcal/mol in the LCCSD case. For the benzene dimer we have 0.29 kcal/mol vs. 1.97 kcal/mol. Hence, a significant portion of the overestimation of E_{int} by LMP2 comes from an underestimation of the repulsive δE_{intra}. Interestingly, this is not amended at all by replacing LMP2 by LCCSD|LMP2, as long as the coupling between LMP2 close pairs, and LCCSD strong pairs remains switched off (LCCSD|LMP2*uc*). Switching on this coupling (the LMP2 close pair amplitudes are now allowed to contribute to the LCCSD strong pair residual) has a large effect: the recommended (coupled) LCCSD|LMP2 approach yields much improved δE_{intra} (whereas the δE_{inter} remain at their LMP2 value). For example, for the π-stacked pyridine and benzene dimers δE_{intra} values of 2.86 and 2.40 kcal/mol are now obtained. The LCCSD reference values are now somewhat overestimated (by 0.5 and 0.4 kcal/mol, respectively, for these two examples) but this favorably compensates partly the too attractive δE_{inter} values. As a result, the LCCSD|LMP2 interaction energies are clearly much superior to those of pure LMP2 for π-stacked systems.

The performance of LCCSD|d-LrCCD is clearly worse than that of LCCSD|LMP2. The main problem is that the δE_{inter} are not attractive enough. Even though the uncoupled LCCSD|d-LrCCD*uc* method provides quite good interaction energies in many cases (cf., e.g., guanine-cytosine (stacked)) this is due to a cancellation of errors between too small attractive δE_{inter}, and too small repulsive δE_{intra}. In the coupled LCCSD|d-LrCCD, on the other hand, this error cancellation is destroyed, leading to grossly underestimated interaction energies for all dimers in Table II.

As already pointed out above, d-LrCCD does not include all diagrams up to a certain order with respect to the fluctuation potential which decay as R^{-6} with the distance R between the the respective LMOs of the close pair. In particular, the third-order diagram D6 is missing, while the third-order diagram D1 is present. This is fixed in the rCCD3 method. As is evident from Table II LCCSD|LrCCD3 is clearly superior to LCCSD|LMP2: E_{int} usually deviates by not more than half a kcal/mol from the LCCSD reference value. Moreover, the individual δE_{intra} and δE_{inter} components are closer to those of LCCSD, indicating that LCCSD|LrCCD3 does not depend as much on fortuitous cancellation of errors in the sum of these two contributions as LCCSD|LMP2 does. The performance of LCCSD|LrCCD, i.e., with inclusion of the fourth order diagrams, is again less good; in particular there is no improvement over LCCSD|LMP2. Note that rCCD again does not comprise all fourth order diagrams which decay as R^{-6}. For example, the CCD diagrams D13–D16 of Fig. 5 are missing. Moreover, there is a contribution to the doubles residual involving singles amplitudes in LCCSD, which of course is omitted in rCCD.

As already mentioned at the end of Sec. II A, close pair amplitudes also enter the L(T) residual. Replacing the LCCSD close pairs in the reference calculation by LMP2 or LrCCD3 close pairs in the LCCSD(T)|LMP2 and LCCSD(T)|LrCCD3 methods therefore affects E_{int} also via its triples contribution ΔE_{T}. Table III compares the results of reference LCCSD(T), LCCSD(T)|LMP2, and LCCSD(T)|LrCCD3 calculations for the test set adopted from the S66 set. Generally, apart from two electrostatically dominated cases the ΔE_{T} values obtained with LCCSD(T)|LrCCD3 are always closer to the corresponding reference than the LCCSD(T)|LMP2 values. Apparently, the LrCCD3 close pair amplitudes mimic those of LCCSD better than the LMP2 ones. This effect is even more articulate for the trimers discussed in Subsection III B (cf. Table V). The consequence of a better ΔE_{T} value is of course a further improvement in E_{int} when comparing LCCSD(T)|LrCCD3 to LCCSD(T)|LMP2. Also relative energies of related systems are considerably improved; the LCCSD(T), LCCSD(T)|LMP2, and LCCSD(T)|LrCCD3 relative energies of π-stacked vs. T-shaped geometries amount to 0.06, −0.63, and −0.23 kcal/mol for the benzene dimer, and −0.21, −1.00, and −0.56 kcal/mol for the pyridine dimer.

B. $(Kr)_3$ and $(CS_2)_3$ trimers

Apart from the dimers of Table II also the trimers $(Kr)_3$ and $(CS_2)_3$ were investigated; the Krypton trimer in equilateral geometry for two interatomic distances R, the $(CS_2)_3$ for two intermolecular distances R, and two tilting angles α. The geometries of the $(CS_2)_3$ trimer are displayed in Fig. 6. $R = 3.811$ Å, $\alpha = 28.2^\circ$ correspond to the observed geometry reported in Ref. 64; $R = 3.65$ Å corresponds to the MP2 minimum structure (aug-cc-pVTZ basis); $\alpha = 0.0^\circ$ corresponds to a parallel arrangement of the CS_2 monomers

TABLE II. Comparison of the intermolecular interaction energies and their components of LCCSD|X to full LCCSD (all pairs strong) with X = LMP2*uc* (for uncoupled), X = d-LrCCD*uc*, X = LMP2, X = d-LrCCD, X = LrCCD3, X = LrCCD for a set of dimers. Correlation contributions ΔE_c to the respective interaction energies, and their intra- and intermolecular components δE_{intra} and δE_{inter}, respectively, all in kcal/mol are also provided. Furthermore, the RMS and maximum deviations relative to the CCSD calculation are given. The prefix "L" for local was omitted in the method names, for brevity. The corresponding complete table containing the entries of all calculations carried out in this work is provided in the supplementary material.[63]

	CCSD	MP2	CCSD| MP2*uc*	CCSD| d-rCCD*uc*	CCSD| MP2	CCSD| d-rCCD	CCSD| rCCD3	CCSD| rCCD
Electrostatic dominated								
Water dimer								
δE_{inter}	−2.318	−2.205	−2.205	−1.863	−2.206	−1.795	−2.324	−2.387
δE_{intra}	1.594	1.277	1.362	1.362	1.593	1.512	1.596	1.605
ΔE_c	−0.724	−0.929	−0.844	−0.501	−0.612	−0.283	−0.727	−0.781
E_{int}	−4.349	−4.554	−4.469	−4.126	−4.238	−3.909	−4.352	−4.406
Guanine-cytosine (Watson Crick)								
δE_{inter}	−13.860	−13.749	−13.749	−11.345	−13.731	−10.854	−14.081	−14.621
δE_{intra}	10.570	9.667	8.880	8.881	10.673	10.002	10.619	10.715
ΔE_c	−3.290	−4.083	−4.869	−2.465	−3.058	−0.852	−3.462	−3.906
E_{int}	−27.729	−28.520	−29.307	−26.904	−27.497	−25.291	−27.901	−28.345
Dispersion dominated								
Pyridine-pyridine (π-π)								
δE_{inter}	−7.707	−9.150	−9.150	−6.486	−9.148	−6.060	−8.344	−8.925
δE_{intra}	2.388	0.567	0.592	0.593	2.857	1.953	2.521	2.685
ΔE_c	−5.319	−8.583	−8.558	−5.893	−6.291	−4.108	−5.823	−6.240
E_{int}	−1.976	−5.241	−5.215	−2.551	−2.948	−0.765	−2.481	−2.898
Pyridine-pyridine (TS)								
δE_{inter}	−5.538	−6.043	−6.043	−4.717	−6.040	−4.436	−5.841	−6.151
δE_{intra}	2.406	1.390	1.436	1.436	2.607	2.139	2.478	2.558
ΔE_c	−3.132	−4.653	−4.607	−3.281	−3.433	−2.297	−3.363	−3.594
E_{int}	−2.254	−3.777	−3.731	−2.405	−2.557	−1.421	−2.487	−2.718
Benzene-benzene(π-π)								
δE_{inter}	−7.035	−8.369	−8.369	−5.891	−8.368	−5.504	−7.672	−8.204
δE_{intra}	1.965	0.293	0.281	0.282	2.397	1.559	2.095	2.246
ΔE_c	−5.070	−8.076	−8.089	−5.609	−5.971	−3.946	−5.577	−5.958
E_{int}	−1.103	−4.110	−4.121	−1.643	−2.003	0.022	−1.609	−1.990
Benzene-benzene (TS)								
δE_{inter}	−5.172	−5.729	−5.729	−4.350	−5.724	−4.086	−5.527	−5.833
δE_{intra}	2.101	1.111	1.113	1.114	2.300	1.835	2.176	2.255
ΔE_c	−3.071	−4.618	−4.616	−3.236	−3.424	−2.251	−3.351	−3.578
E_{int}	−1.618	−3.163	−3.159	−1.781	−1.969	−0.796	−1.896	−2.123
Guanine-cytosine (stacked)								
δE_{inter}	−18.237	−20.212	−20.212	−15.028	−20.212	−14.140	−18.724	−19.827
δE_{intra}	9.193	6.752	5.932	5.931	9.834	8.193	9.242	9.514
ΔE_c	−9.045	−13.460	−14.280	−9.098	−10.378	−5.947	−9.482	−10.313
E_{int}	−14.455	−18.875	−19.699	−14.514	−15.790	−11.360	−14.895	−15.725
Mixed								
Uracil-uracil (π-π)								
δE_{inter}	−11.953	−13.078	−13.078	−9.569	−13.067	−8.972	−12.297	−12.996
δE_{intra}	4.867	2.844	2.695	2.695	5.202	4.141	4.870	5.041
ΔE_c	−7.086	−10.235	−10.383	−6.874	−7.865	−4.831	−7.427	−7.955
E_{int}	−6.684	−9.833	−9.982	−6.475	−7.464	−4.431	−7.026	−7.554
RMS deviation								
δE_{inter}		0.900	0.900	1.613	0.899	2.021	0.363	0.846
δE_{intra}		1.921	1.545	1.545	0.293	0.467	0.065	0.180
ΔE_c		2.591	2.380	0.389	0.613	1.558	0.303	0.667
E_{int}		2.194	2.381	0.389	0.613	1.557	0.304	0.668
Maximum deviation								
δE_{inter}		1.975	1.975	3.209	1.975	4.097	0.637	1.590
δE_{intra}		5.381	3.261	3.262	0.642	1.000	0.134	0.322
ΔE_c		5.397	5.235	0.825	1.333	3.097	0.506	1.268
E_{int}		4.420	5.244	0.825	1.335	3.095	0.506	1.270

TABLE III. Intermolecular interaction energies E_{int}, correlation contributions of the local triples correction, ΔE_T (all in kcal/mol). The RMS and maximum deviations relative to the LCCSD(T0) calculation are also given. The prefix "L" for local was omitted in the method names, for brevity. The corresponding complete table containing the entries of all calculations carried out in this work is provided in the supplementary material.[63]

	CCSD(T)	CCSD(T)|MP2	CCSD(T)|rCCD3
	Electrostatic dominated		
	Water dimer		
E_{int}	−4.522	−4.390	−4.524
ΔE_T	−0.173	−0.152	−0.172
	Dispersion dominated		
	Pyridine-pyridine (π-π)		
E_{int}	−3.065	−4.327	−3.719
ΔE_T	−1.089	−1.379	−1.238
	Pyridine-pyridine (TS)		
E_{int}	−2.857	−3.267	−3.161
ΔE_T	−0.603	−0.710	−0.674
	Benzene-benzene (π-π)		
E_{int}	−2.158	−3.323	−2.811
ΔE_T	−1.055	−1.320	−1.202
	Benzene-benzene (TS)		
E_{int}	−2.220	−2.691	−2.578
ΔE_T	−0.602	−0.722	−0.682
	Mixed		
	Uracil-uracil (π-π)		
E_{int}	−8.252	−9.188	−8.685
ΔE_T	−1.568	−1.724	−1.659
	RMS deviation		
E_{int}		0.773	0.389
ΔE_T		0.161	0.086
	Maximum deviation		
E_{int}		1.663	0.654
ΔE_T		0.328	0.149

in the trimer. In all the calculations the C–S bond length was fixed at 1.565 Å, obtained by a CCSD(T)/cc-pVTZ optimization of the CS_2 monomer.

The calculated interaction energies E_{int}, the correlation contributions ΔE_c thereof, and the three-body correlation contributions ΔE_{3c} are collected in Table IV. For the interaction energies of Kr_3 the same trend is observed as for the dimers: LMP2 yields too attractive E_{int}, which is amended by LCCSD|LMP2 to large extent; LCCSD|LrCCD3 is a clear improvement over LCCSD|LMP2, and LCCSD|LrCCD again

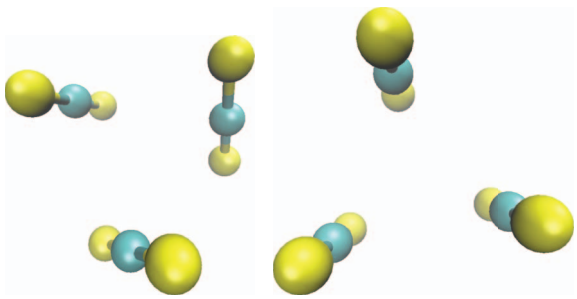

$\alpha = 28.2°$ $\alpha = 0.0°$

FIG. 6. $(CS_2)_3$ trimer geometry for two tilting angles α.

TABLE IV. Intermolecular interaction energies E_{int}, correlation contributions ΔE_c to E_{int}, and three-body correlation contributions ΔE_{3c} to ΔE_c (all in kcal/mol) of equilateral Kr_3 and $(CS_2)_3$ for different interatomic or intermolecular distances R (in Å). For $(CS_2)_3$, two different tilting angles α were applied: $\alpha = 28.2°$, $R = 3.811$ Å is the experimental geometry reported in Ref. 64, and $\alpha = 0°$ specifies a parallel arrangement of the three CS_2 molecules. $R = 3.65$ Å corresponds to the MP2 minimum. The prefix "L" for local was omitted in the method names, for brevity.

	R	CCSD	MP2	CCSD|MP2	CCSD|rCCD3	CCSD|rCCD
			Equilateral Kr_3			
E_{int}	5.0	−0.385	−0.513	−0.403	−0.371	−0.399
E_{int}	4.0	−0.463	−0.985	−0.573	−0.445	−0.561
ΔE_c	4.0	−1.724	−2.246	−1.834	−1.706	−1.822
ΔE_{3c}	4.0	0.024	0.013	0.011	0.031	0.030
			Equilateral $(CS_2)_3$, $\alpha = 28.2°$			
E_{int}	3.81	−3.018	−8.924	−4.913	−3.668	−4.556
E_{int}	3.65	−1.899	−9.299	−4.266	−2.654	−3.763
ΔE_c	3.81	−8.297	−14.203	−10.192	−8.946	−9.835
ΔE_c	3.65	−10.371	−17.771	−12.739	−11.127	−12.235
ΔE_{3c}	3.81	0.172	0.096	0.052	0.275	0.267
ΔE_{3c}	3.65	0.254	0.167	0.097	0.392	0.384
			Equilateral $(CS_2)_3$, $\alpha = 0°$			
E_{int}	3.81	−0.328	−6.849	−2.404	−1.026	−2.040
E_{int}	3.65	2.340	−5.887	−0.269	1.525	0.259
ΔE_c	3.81	−9.261	−15.782	−11.338	−9.960	−10.974
ΔE_c	3.65	−11.723	−19.949	−14.332	−12.538	−13.803
ΔE_{3c}	3.81	0.303	0.188	0.110	0.464	0.459
ΔE_{3c}	3.65	0.452	0.321	0.203	0.665	0.662

is in the same ballpark as LCCSD|LMP2. The three-body correlation contributions amount to about 1.5% of the total correlation contribution to E_{int}; they are underestimated by LMP2 and LCCSD|LMP2 (Axilrod-Teller terms are of third order and therefore not included), and somewhat overestimated by LCCSD|LrCCD3 and LCCSD|LrCCD.

For the $(CS_2)_3$ trimer MP2 is particularly bad, e.g., at the experimental geometry, E_{int} is overestimated by 6 kcal/mol. LCCSD|LMP2 still overestimates the LCCSD value by almost 2 kcal/mol, while for LCCSD|LrCCD3 the error reduces to somewhat more than half a kcal/mol. LCCSD|LrCCD again is worse, but still better than LCCSD|LMP2. The three-body correlation contributions amount to 2% (tilted geometry) and 3% (parallel geometry) of ΔE_c for $R = 3.811$ Å. Again, LMP2 and LCCSD|LMP2 underestimate the LCCSD ΔE_{3c} values, while LCCSD|LrCCD3 and LCCSD|LrCCD overestimate it.

Finally, Table V compares the results of reference LCCSD(T), LCCSD(T)|LMP2, and LCCSD(T)|LrCCD3 calculations on the $(CS_2)_3$ trimer. Evidently, ΔE_T is quite important for this system; for the experimental geometry it amounts to almost 2 kcal/mol, and for the other geometries somewhat more. The LCCSD(T)|LMP2 method overestimates ΔE_T by about half a kcal/mol, while LCCSD(T)|LrCCD3 yields a very accurate value. Again, it appears that the LrCCD3 close pair amplitudes are a better approximation of the corresponding LCCSD amplitudes than the LMP2 ones. As a result, LCCSD(T)|LMP2 overestimates E_{int} of the experimental geometry by 2.5 kcal/mol, while the error reduces to less than

TABLE V. Intermolecular interaction energies E_{int}, correlation contributions of the local triples correction, ΔE_{T} (all in kcal/mol) of $(CS_2)_3$ for two different interatomic or intermolecular distances R (in Å) and two different tilting angles α. $R = 3.811$Å, $\alpha = 28.2^\circ$ is the experimental geometry reported in Ref. 64, $R = 3.65$ Å corresponds to the LMP2 minimum, and $\alpha = 0^\circ$ to a parallel arrangement of the three CS_2 molecules. In parentheses the differences of the individual E_{int} relative to the experimental geometry are given. The prefix "L" for local was omitted in the method names, for brevity.

	R	CCSD(T)	CCSD(T)|MP2	CCSD(T)|rCCD3
		Equilateral $(CS_2)_3$, $\alpha = 28.2^\circ$		
E_{int}	3.81	− 4.948 (0.00)	− 7.424 (0.00)	− 5.766 (0.00)
E_{int}	3.65	− 4.267 (0.68)	− 7.362(0.06)	− 5.218 (0.55)
ΔE_{T}	3.81	− 1.930	− 2.511	− 2.098
ΔE_{T}	3.65	− 2.368	− 3.096	− 2.564
		Equilateral $(CS_2)_3$, $\alpha = 0^\circ$		
E_{int}	3.81	− 2.534 (2.41)	− 5.317 (2.11)	− 3.422 (2.34)
E_{int}	3.65	− 0.394 (4.55)	− 3.889 (3.54)	− 1.434 (4.33)
ΔE_{T}	3.81	− 2.206	− 2.913	− 2.396
ΔE_{T}	3.65	− 2.734	− 3.620	− 2.959

a kcal/mol for LCCSD(T)|LrCCD3. Moreover, as is also evident from Table V, the relative energies of the four geometries obtained with LCCSD(T)|LrCCD3 are in much closer agreement with the reference than those of LCCSD(T)|LMP2.

C. Linear Gly_4 chain

In order to compare the LCCSD(T)|LrCCD3 vs. LCCSD(T)|LMP2 treatment of *intramolecular* close and weak pairs we present in Table VI calculations on the linear poly-glycine peptide chain $(Gly)_4$, $HO[C(O)CH_2NH]_4H$. The geometry can be found in the supplementary material of Ref. 6. For these calculations the strong, close, and weak pairs were specified by the two distance thresholds R_c and R_w: pairs with interorbital distances $R < R_c$, $R_c \leq R < R_w$, and $R_w \leq R$ are considered as strong, close, and weak, respectively. Table VI compares LCCSD correlation energies E_{CCSD} and L(T0) triples corrections E_{T}, obtained with LCCSD(T)|LMP2 (uncoupled and coupled) and LCCSD(T)|LrCCD3 (coupled) for different settings of R_c and R_w. Evidently, the E_{CCSD} values obtained with LCCSD(T)|LrCCD3 are in much better agreement with the full LCCSD(T) reference value than those of the related LCCSD(T)|LMP2 calculation. For $(R_c, R_w) = (1, 3)$ bohr the deviation from the reference amounts to −10 and 2 mH for LCCSD(T)|LMP2 and LCCSD(T)|LrCCD3, respectively. For LCCSD(T)|LMP2 the overestimation of E_{CCSD} fortuitously cancels to large extent with the underestimated E_{T} value, since for $R_w = 3$ bohrs the local triples list (formed from strong and close pairs only[3]) still is rather short. Increasing the number of close pairs by setting R_w to 8 bohrs reduces the deviations from the reference E_{CCSD} value to −5 mH and −0.1 mH, respectively. With such a setting E_{T} is still underestimated by about 1 mH. Apparently, the convergence of E_{CCSD} with increasing number of close pairs is quicker than that of E_{T}. Consequently, one may consider to decouple the construction of the orbital triples list from the criterion of coupling strong and close pairs in the amplitude equations.

TABLE VI. CCSD correlation energies E_{CCSD} and corresponding triples corrections E_{T} (all in hartree) for the linear Gly_4 chain with different specifications for the pair approximation. LCCSD(T0)|X with X = LrCCD3, X = LMP2, and X = LMP2*uc* (for uncoupled) are compared to a full LCCSD(T0) calculation (all pairs strong). The number of strong, close, and weak pairs, as well as the number of orbital triples is also given. Furthermore, the average elapsed times per iteration T_{avg} (in s) is provided for each method. Convergence was always reached in nine iterations.

R_c	R_w	Number of strong|close|weak pairs	Number of orbital triples	E_{T}	E_{CCSD}	T_{avg}
			LCCSD(T0)|MP2*uc*			
1	3	173 | 140 | 863	1197	− 0.138429	− 3.356354	211
1	8	173 | 439 | 564	3420	− 0.148418	− 3.356352	314
4	8	313 | 299 | 564	4458	− 0.145835	− 3.335908	590
8	18	612 | 387 | 177	13101	− 0.145289	− 3.330224	1652
9	28	636 | 540 | 0	18617	− 0.145291	− 3.330197	1840
			LCCSD(T0)|MP2			
1	3	173 | 140 | 863	1197	− 0.135811	− 3.340167	456
1	8	173 | 439 | 564	3420	− 0.144770	− 3.334735	624
4	8	313 | 299 | 564	4458	− 0.144932	− 3.330585	882
8	18	612 | 387 | 177	13101	− 0.145274	− 3.330125	2024
9	28	636 | 540 | 0	18617	− 0.145281	− 3.330130	2267
			LCCSD(T0)|rCCD3			
1	3	173 | 140 | 863	1197	− 0.135279	− 3.327975	552
1	8	173 | 439 | 564	3420	− 0.144021	− 3.330273	745
4	8	313 | 299 | 564	4458	− 0.144921	− 3.330367	980
8	18	612 | 387 | 177	13101	− 0.145291	− 3.330156	2149
9	28	636 | 540 | 0	18617	− 0.145297	− 3.330161	2310
			Full LCCSD(T0)			
		1176 | 0 | 0	19552	− 0.145292	− 3.330191	4272

Table VI also compiles the average wall clock times per iteration for the different calculations. The calculations were carried out on four Intel Xeon cores X5560@2.8 GHz. Evidently, the additional computational cost on going from the coupled LCCSD(T)|LMP2 to the LCCSD(T)|LrCCD3 treatment of close and weak pair is quite small, i.e., about 20% for $R_c = 1$ bohr, and considerably less if the number of strong pairs is increased. LCCSD(T)|LrCCD3 thus still is a computationally economic method and can easily be applied to any system accessible to LCCSD(T)|LMP2.

IV. CONCLUSIONS

In local correlation approaches like the local CCSD(T) method the reduction of the number of determinants and related amplitudes is based on (i) the truncation of the virtual space to pair or triple specific subspaces, and (ii) truncations of the pair list of localized occupied orbitals (pair approximations). The former exploits an exponential, the later a polynomial R^{-6} decay of the pair energies with respect to the distance R between the corresponding localized orbitals. Obviously, the pair approximation is more critical and needs some care. In a LCCSD(T) treatment, pairs with larger R, i.e., close and weak pairs are not simply neglected but treated at a lower level of theory, typically local MP2, while only strong pairs enjoy the full CC treatment. Yet a MP2 treatment of close and weak pairs may not provide sufficient accuracy, for

example, if the system comprises π stacked aromatic rings, or in other situations where van der Waals contributions play a significant role. In this article we have investigated the effect of different pair approximations for a test set of intermolecular dimers and trimers. We compare a MP2 treatment of close and weak pairs to alternatives based on the ring-CCD method where 3rd or 4th order diagrams with intermolecular R^{-6} decay are also included. It turns out that the coupling between close and strong pairs, i.e., the feedback of close pair amplitudes in the strong pair LCCSD amplitude equations, and vice versa, the feedback of strong pair amplitude equations in the weak + close amplitude equations is essential (the latter only for LrCCDn, but not for LMP2). The coupled LCCSD(T)|LMP2 approach provides much better interaction energies than un-coupled LCCSD(T)|LMP2 or pure LMP2. Interestingly, the improvement is almost exclusively due to an improved description of the repulsive intramolecular contribution, which is significantly underestimated by un-coupled LCCSD(T)|LMP2 or pure LMP2. Part of the success of coupled LCCSD(T)|LMP2 comes from a fortuitous cancellation between intra- and intermolecular contributions to the correlation energy.

A significant improvement in the accuracy over coupled LCCSD(T)|LMP2, subject to only an insignificant increase in the computational cost, is achieved when the LMP2 treatment of close/weak pairs is replaced by ring-LCCD3, i.e., all R^{-6} decaying ring-CCD diagrams up to third-order in the fluctuation potential are included. Such a (coupled) LCCSD(T)|LrCCD3 scheme is clearly superior to LCCSD(T)|LMP2 for van-der Waals dominated systems, and about as good for H-bonded systems. A direct-rCCD treatment of close/weak pairs, on the other hand, yields only disappointing results. It turned out that a third-order diagram absent in direct-rCCD, but present in LrCCD3, is vital for a proper description of close/weak pairs. On the basis of this work we recommend to substitute LCCSD(T)|LMP2 by LCCSD(T)|LrCCD3 in future local CCSD(T) applications.

ACKNOWLEDGMENTS

Financial support of the Deutsche Forschungsgemeinschaft (DFG), Grant Nos. US-103/1-1 (D. Usvyat) and SCHU 1456/3-2 (M. Schütz), is gratefully acknowledged.

[1] J. Cizek, J. Chem. Phys. **45**, 4256 (1966).
[2] R. J. Bartlett and M. Musiał, Rev. Mod. Phys. **79**, 291 (2007).
[3] M. Schütz, J. Chem. Phys. **113**, 9986 (2000).
[4] M. Schütz and H.-J. Werner, Chem. Phys. Lett. **318**, 370 (2000).
[5] H.-J. Werner and M. Schütz, J. Chem. Phys. **135**, 144116 (2011).
[6] M. Schütz, J. Yang, G. K. L. Chan, F. R. Manby, and H.-J. Werner, J. Chem. Phys. **138**, 054109 (2013).
[7] P. E. Maslen, A. Dutoi, M. S. Lee, Y. H. Shao, and M. Head-Gordon, Mol. Phys. **103**, 425 (2005).
[8] W. Li, P. Piecuch, J. R. Gour, and S. Li, J. Chem. Phys. **131**, 114109 (2009).
[9] Z. Rollik and M. Kállay, J. Chem. Phys. **135**, 104111 (2011).
[10] J. Pipek and P. G. Mezey, J. Chem. Phys. **90**, 4916 (1989).
[11] S. F. Boys, "Localized orbitals and localized adjustment functions," in *Quantum Theory of Atoms, Molecules, and the Solid State*, edited by P. O. Löwdin (Academic Press, New York, 1966), pp. 253–262.
[12] P. Pulay, Chem. Phys. Lett. **100**, 151 (1983).
[13] S. Saebø and P. Pulay, Chem. Phys. Lett. **113**, 13 (1985).
[14] P. Pulay and S. Saebø, Theor. Chim. Acta **69**, 357 (1986).
[15] M. Schütz, G. Hetzer, and H.-J. Werner, J. Chem. Phys. **111**, 5691 (1999).
[16] D. Kats, D. Usvyat, and M. Schütz, Phys. Chem. Chem. Phys. **10**, 3430 (2008).
[17] C. Pisani, M. Schütz, S. Casassa, D. Usvyat, L. Maschio, M. Lorenz, and A. Erba, Phys. Chem. Chem. Phys. **14**, 7615 (2012).
[18] J. Yang, Y. Kurashige, F. R. Manby, and G. K. L. Chan, J. Chem. Phys. **134**, 044123 (2011).
[19] Y. Kurashige, J. Yang, G. K. L. Chan, and F. R. Manby, J. Chem. Phys. **136**, 124106 (2012).
[20] J. Yang, G. K.-L. Chan, F. R. Manby, M. Schutz, and H.-J. Werner, J. Chem. Phys. **136**, 144105 (2012).
[21] D. Kats and F. R. Manby, J. Chem. Phys. **138**, 144101 (2013).
[22] W. Meyer, Int. J. Quantum Chem. **S5**, 341 (1971).
[23] W. Meyer, J. Chem. Phys. **58**, 1017 (1973).
[24] R. Ahlrichs, F. Driessler, H. Lischka, V. Staemmler, and W. Kutzelnigg, J. Chem. Phys. **62**, 1235 (1975).
[25] F. Neese, F. Wennmohs, and A. Hansen, J. Chem. Phys. **130**, 114108 (2009).
[26] F. Neese, A. Hansen, and D. G. Liakos, J. Chem. Phys. **131**, 064103 (2009).
[27] A. Hansen, D. G. Liakos, and F. Neese, J. Chem. Phys. **135**, 214102 (2011).
[28] C. Hättig, D. P. Tew, and B. Helmich, J. Chem. Phys. **136**, 204105 (2012).
[29] C. Krause and H.-J. Werner, Phys. Chem. Chem. Phys. **14**, 7591 (2012).
[30] M. Schütz and H.-J. Werner, J. Chem. Phys. **114**, 661 (2001).
[31] R. Martinez-Casado, G. Mallia, D. Usvyat, L. Maschio, S. Casassa, M. Schütz, and N. Harrison, J. Chem. Phys. **134**, 014706 (2011).
[32] D. Usvyat, K. Sadeghian, L. Maschio, and M. Schütz, Phys. Rev. B **86**, 045412 (2012).
[33] A. Heßelmann, J. Chem. Phys. **128**, 144112 (2008).
[34] R. Sedlak, T. Janowski, M. Pitok, J. ez, P. Pulay, and P. Hobza, J. Chem. Theory Comput. **9**, 3364 (2013).
[35] C. Hampel and H.-J. Werner, J. Chem. Phys. **104**, 6286 (1996).
[36] C. Riplinger and F. Neese, J. Chem. Phys. **138**, 034106 (2013).
[37] W. Li and P. Piecuch, J. Phys. Chem. A **114**, 6721 (2010).
[38] D. L. Freeman, Phys. Rev. B **15**, 5512 (1977).
[39] G. E. Scuseria, T. M. Henderson, and D. C. Sorensen, J. Chem. Phys. **129**, 231101 (2008).
[40] J. Toulouse, W. Zhu, A. Savin, G. Jansen, and J. G. Angyan, J. Chem. Phys. **135**, 084119 (2011).
[41] A. Grüneis, private communication (2008).
[42] J. Paier, B. G. Janesko, T. M. Henderson, G. E. Scuseria, A. Gruneis, and G. Kresse, J. Chem. Phys. **132**, 094103 (2010).
[43] E. J. Baerends, D. E. Ellis, and P. Ros, Chem. Phys. **2**, 41 (1973).
[44] J. L. Whitten, J. Chem. Phys. **58**, 4496 (1973).
[45] O. Vahtras, J. Almlöf, and M. W. Feyereisen, Chem. Phys. Lett. **213**, 514 (1993).
[46] F. R. Manby, J. Chem. Phys. **119**, 4607 (2003).
[47] M. Schütz and F. R. Manby, Phys. Chem. Chem. Phys. **5**, 3349 (2003).
[48] H.-J. Werner, F. R. Manby, and P. J. Knowles, J. Chem. Phys. **118**, 8149 (2003).
[49] F. Weigend, M. Kattannek, and R. Ahlrichs, J. Chem. Phys. **130**, 164106 (2009).
[50] T. S. Chwee and E. A. Carter, J. Chem. Phys. **132**, 074104 (2010).
[51] M. Schütz, H.-J. Werner, R. Lindh, and F. R. Manby, J. Chem. Phys. **121**, 737 (2004).
[52] D. Kats, T. Korona, and M. Schütz, J. Chem. Phys. **125**, 104106 (2006).
[53] D. Kats, T. Korona, and M. Schütz, J. Chem. Phys. **127**, 064107 (2007).
[54] D. Usvyat, "Intermolecular interactions in the local correlation energy partitioning" (unpublished).
[55] R. J. Bartlett and J. Noga, Chem. Phys. Lett. **150**, 29 (1988).
[56] D. Kats, D. Usvyat, and M. Schütz, Phys. Rev. A **83**, 062503 (2011).
[57] J. Řezáč, K. E. Riley, and P. Hobza, J. Chem. Theory Comput. **7**, 2427 (2011).
[58] T. H. Dunning, Jr., J. Chem. Phys. **90**, 1007 (1989).
[59] R. A. Kendall, T. H. Dunning, and R. J. Harrison, J. Chem. Phys. **96**, 6796 (1992).
[60] F. Weigend, M. Häser, H. Patzelt, and R. Ahlrichs, Chem. Phys. Lett. **294**, 143 (1998).
[61] M. Schütz, G. Rauhut, and H.-J. Werner, J. Phys. Chem. A **102**, 5997 (1998).
[62] J. W. Boughton and P. Pulay, J. Comput. Chem. **14**, 736 (1993).
[63] See supplementary material at http://dx.doi.org/10.1063/1.4826534 for the results of the calculations on an extended set of systems.
[64] M. Rezaei, J. Norooz Oliaee, N. Moazzen-Ahmadi, and A. R. W. McKellar, Phys. Chem. Chem. Phys. **13**, 12635 (2011).